Synergistic Impacts of the Atlantic and Pacific Oceans on Interdecadal Variations of Summer Rainfall in Northeast Asia

Dong SI[1,2*], Dabang JIANG[1,3], and Yihui DING[4]

1 *Climate Change Research Center*, *Institute of Atmospheric Physics*, *Chinese Academy of Sciences*, *Beijing* 100029
2 *Collaborative Innovation Center on Forecast and Evaluation of Meteorological Disasters*, *Nanjing University of Information Science & Technology*, *Nanjing* 210044
3 *College of Earth and Planetary Sciences*, *University of Chinese Academy of Sciences*, *Beijing* 100049
4 *National Climate Center*, *China Meteorological Administration*, *Beijing* 100081

(Received November 18, 2020; in final form June 2, 2021)

ABSTRACT

This study presents a comprehensive analysis of the synergistic impacts of the Atlantic multidecadal oscillation (AMO) and Pacific decadal oscillation (PDO) on the interdecadal variations of summer rainfall in Northeast Asia. Following the construction of four probable scenarios under various combinations of the AMO and PDO phases, it is found that when the AMO and PDO are out of phase, both of them induce a strong or weak East Asian summer monsoon and a low or high pressure system over Northeast Asia through atmospheric teleconnection, which results in significant wet or dry conditions over the whole of Northeast Asia through the effects of superimposition. In contrast, when the AMO and PDO are in-phase, they induce moderate and regional wet or dry conditions in Northeast Asia, and only a slightly strong or weak East Asian summer monsoon through the effects of cancellation. During the mid-1960s–1990s, a period of drought first began in Northeast Asia under a negative AMO and negative PDO in the mid-1960s, which then increased in severity under a negative AMO and positive PDO in the 1980s, before finally coming to an end under a positive AMO and negative PDO in the late 1990s. The interdecadal predictability of summer rainfall in Northeast Asia may reside in the interdecadal behavior of the North Atlantic and Pacific Oceans.

Key words: Atlantic multidecadal oscillation, Pacific decadal oscillation, synergistic impacts, Northeast Asia, summer rainfall

Citation: Si, D., D. B. Jiang, and Y. H. Ding, 2021: Synergistic impacts of the Atlantic and Pacific Oceans on interdecadal variations of summer rainfall in Northeast Asia. *J. Meteor. Res.*, **35**(5), 844–856, doi: 10.1007/s13351-021-0191-2.

1. Introduction

The importance of decadal to interdecadal climate changes has been increasingly recognized over recent decades, including by the Intergovernmental Panel on Climate Change (IPCC) and World Climate Research Programme (WCRP). An improved understanding of decadal to interdecadal climate changes is very important because policymakers want to know the likely climate status for the coming decades so that they can plan for the mitigation and adaptation of the potential threat from climate changes.

Northeast Asia is not only one of the world's main population centers, but also one of its main agricultural production and industrial regions. The urgency for a scientific understanding of interdecadal climate change in Northeast Asia became evident following the persistent drought experienced in the region from the mid-1960s (Ma and Fu, 2006; Kim et al., 2011). Northeast Asia is situated at the northern edge of the East Asian summer monsoon region. It is influenced by both the low-latitude and high-latitude atmospheric circulations (Lee et al., 2005; Liu et al., 2010). At the mid–high latitudes, cold vortex over Northeast Asia and blocking activities over the Okhotsk Sea occur frequently, associated with Rossby wave propagation (Bueh et al., 2016; Xie and

Supported by the National Natural Science Foundation of China (41875104 and 41991284) and Strategic Priority Research Program of the Chinese Academy of Sciences (XDA20100304).

*Corresponding author: sidong@mail.iap.ac.cn

Bueh, 2017) and atmospheric teleconnection (Liu et al., 2012, 2020). At the mid–low latitudes, the northward advance of the East Asian summer monsoon as well as its subsystems, such as the western North Pacific subtropical high and the water vapor transport, affects the climate in Northeast Asia (Piao et al., 2021). Due to the unique geographic location and the complex synoptic and climatic characteristics, predictability of the Northeast Asian climate variability is low (Gao et al., 2014).

Observational evidence indicates that the summertime climate of Northeast Asia has experienced remarkable interdecadal changes, induced by both natural variability and anthropogenic forcings (Jiang and Wang, 2005; Ha et al., 2020). For instance, it is suggested that aerosol-induced tropospheric cooling over Asian land areas weakens the East Asian summer monsoon north of 20°N and decreases the summer rainfall over Northeast Asia (Wang et al., 2019). Decadal to multidecadal oceanic variabilities have been shown to affect the interdecadal change of Northeast Asian rainfall (Ding et al., 2009; Qin et al., 2018; Zhou et al., 2020). In the Pacific Ocean, this variability is referred to as the Pacific decadal oscillation (PDO), while in the Atlantic Ocean it is referred to as the Atlantic multidecadal oscillation (AMO).

The PDO, which is defined as the leading principal component of North Pacific sea surface temperature (SST) variability poleward of 20°N (Mantua et al., 1997), has been found to relate closely to the interdecadal changes of the East Asian summer monsoon and Northeast Asian summer rainfall. The negative phase of PDO favors an enhanced East Asian monsoon and Northeast Asian rainfall during summer, while the opposite trends hold during its positive phase (Zhu and Yang, 2003; Ma, 2007; Gong et al., 2016; Zheng et al., 2017; Ding et al., 2020). The negative phase of PDO corresponds to warm SSTs over the tropical western Pacific Ocean, which triggers a meridional wave train extending from the tropical western Pacific to Northeast Asia along the East Asian coast. Northeast Asia is dominated by an anomalous low pressure in the middle troposphere and an anomalous cyclone in the lower troposphere, which favors above-normal summer rainfall in Northeast Asia (Qian and Zhou, 2014; Si and Ding, 2016). Moreover, an enhanced land–sea thermal contrast in East Asia–Pacific sector during the negative phase of PDO strengthens the East Asian summer monsoon, which also contributes to the wet conditions in Northeast Asia (Qian and Zhou, 2014).

The AMO, which is defined as the mean of Atlantic detrended SST anomalies north of the equator (Schlesinger and Ramankutty, 1994), has significant influences on climate fluctuations in many regions of the Northern Hemisphere, including Europe and North America (Sutton and Hodson, 2005; Sutton and Dong, 2012; Wu et al., 2016; Zhou and Wu, 2016), North Africa (Ting et al., 2011), South Asia (Luo et al., 2011; Yan et al., 2018; Nath and Luo, 2019), and Southeast Asia (Fan et al., 2019). The AMO affects the summer monsoon and rainfall in East Asia, with its positive phase leading to strong summer monsoon over East Asia and high temperature and excessive rainfall over East China (Li et al., 2017; Zhang et al., 2018; Jiang et al., 2020). The positive phase of AMO leads to a strong East Asian summer monsoon through atmosphere–ocean coupling in the western Pacific–Indian Ocean sector and tropospheric temperature changes over Eurasian continent (Lu et al., 2006). Other studies suggest that the AMO can influence the global surface temperature and ocean heat redistribution (Hu et al., 2018) as well as the climate effect of the Tibetan Plateau (Lu et al., 2019). A recent study has shown that the AMO affects Northeast Asia via a circumglobal teleconnection pattern. This teleconnection includes seven action centers over the North Atlantic, western Europe, eastern Europe, central Asia, Lake Baikal, East Asia, and the North Pacific in order (Si and Ding, 2016). The positive phase of AMO favors the occurrence of cold vortex over Northeast Asia and blocking over western North Pacific through the circumglobal teleconnection, which enhances the East Asian summer monsoon and southward intrusion of cold air from high-latitude, and leads to above-normal summer rainfall in Northeast Asia (Si et al., 2021).

The impacts of the PDO and AMO on the summer climate in East Asia have been considered separately in nearly all previous works, with little attention having been paid to their synergistic impacts. Therefore, in this study, our aim is to analyze how the summer rainfall variation in Northeast Asia is influenced by synergistic impacts of both the PDO and AMO. The paper is organized as follows. Section 2 introduces the observational data, method, model, and experiments. Section 3 analyzes the temporal fluctuations of the PDO and AMO. In Sections 4 and 5, we analyze the composites of summer rainfall and the monsoon over Northeast Asia under varying PDO and AMO regimes, respectively. Finally, Section 6 provides a summary of our findings and further discussion.

2. Data, method, model, and experiment

2.1 *Data and method*

The gridded precipitation dataset is from the Climate Research Unit (CRU) (CRU–TS_3.26), and covers

1901–2017. The other precipitation dataset is a 113-yr-long station precipitation dataset (Wang et al., 2000), of which 11 stations (Taiyuan, Beijing, Jinan, Yantai, Zhengzhou, Xuzhou, Xinyang, Chaoyang, Shenyang, Changchun, and Harbin) are used to represent the interdecadal variation of summer precipitation in Northeast Asia. Atmospheric data are from the NOAA 20th century global reanalysis, version 2 (NOAA–20C) (Compo et al., 2011), including the 500-hPa geopotential height, 850-hPa zonal and meridional wind components, and 850-hPa specific humidity. Monthly mean SST data are from a merged product of the Hadley Centre and NOAA's optimum interpolation SST dataset (Hurrell et al., 2008).

The PDO index is defined as the time coefficient of the leading empirical orthogonal function (EOF) mode of North Pacific (20°–70°N, 110°E–100°W) June–July–August (JJA) mean SST. Prior to the EOF analysis, the linear trend is removed from the SST time series at each grid point. The AMO index is expressed as the locally detrended JJA mean SST anomalies averaged over the North Atlantic (0°–60°N, 0°–80°W). To emphasize the interdecadal signal, a low-pass symmetric filter with a 13-yr cutoff period is applied to the PDO and AMO indices.

2.2 *Model and experiment*

To further quantify the fidelity of state-of-the-art coupled Earth system models in simulating the synergistic impacts of the PDO and AMO, we analyze a large ensemble simulation from the Community Earth System Model (CESM-LE). All simulations are performed with the nominal 1° latitude/longitude version of the Community Earth System Model, version 1 (CESM1; Hurrell et al., 2013), with Community Atmosphere Model, version 5.2 (CAM5.2) as its atmospheric component. The CESM-LE simulation includes a 40-member ensemble of fully coupled CESM1 simulations from 1920 to 2100. Each member is forced by the same time-evolving external forcing from 1920 to 2005 and by the representative concentration pathway 8.5 (RCP8.5) scenario from 2006 to 2100 (Kay et al., 2015).

3. Temporal variations of the PDO and AMO

Different from other ocean basins whose leading SST variabilities are characterized by interannual variability, the North Atlantic and extratropical North Pacific are dominated by SST variability at decadal to multidecadal timescales. As shown in Fig. 1, the PDO and AMO indices have exhibited remarkable interdecadal variability since the 1900s. The PDO phase is negative from the late 1900s to the mid-1920s and from the mid-1940s to the late 1970s, but positive from the late 1920s to the early 1940s and from the early 1980s to the 1990s. The PDO phase has been negative since the late 1990s. The AMO phase is negative from the 1900s to the mid-1920s, and from the early 1960s to the late 1990s, but positive from the mid-1920s to the late 1950s and from the late 1990s to the 2010s.

The summer rainfall over Northeast Asia shows a remarkable interdecadal variation from 1900 to 2012 (Fig. 2). Generally, it was above normal during the mid-1900s–mid-1910s, but below normal during the mid-1910s–early 1920s. Since the mid-1940s, the Northeast Asian summer rainfall increased and reached maximum during the 1950s–early 1960s, and decreased rapidly after the mid-1960s. During the 1980s–1990s, the summer rainfall over Northeast Asia changed to below normal, agreeing with a prominent drought over Northeast Asia (Ma, 2007; Kim et al., 2011). Since the late 1990s, the

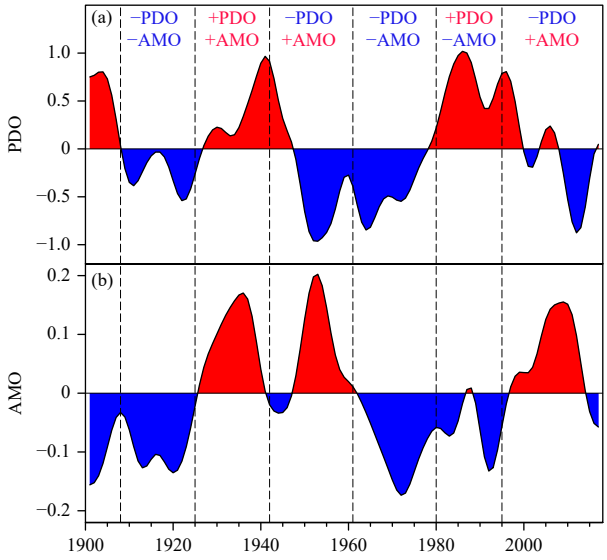

Fig. 1. Time series of the (a) PDO and (b) AMO (°C) indices showing four combinations of PDO and AMO phases.

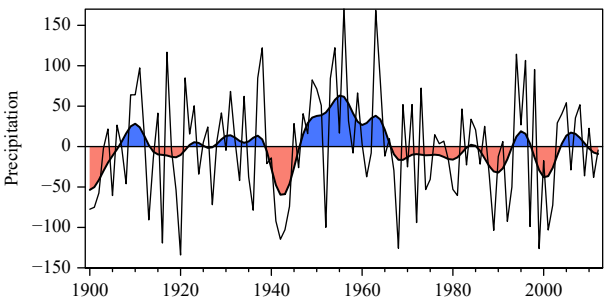

Fig. 2. Time series of anomalous summer precipitation (mm) averaged over 11 stations in Northeast Asia from 1900 to 2012. The filling curve is the decadal-filtered values.

summer rainfall increased over Northeast Asia. From the mid-1960s to 1990s, a period of drought began in Northeast Asia under a negative AMO (−AMO) and negative PDO (−PDO) in the mid-1960s, which then increased in severity under a −AMO and positive PDO (+PDO) in the 1980s, before finally coming to an end under a positive AMO (+AMO) and −PDO in the late 1990s.

According to the PDO and AMO indices, we identified the positive and negative PDO and AMO phases (Fig. 1). Four categories are classified: (1) +PDO and +AMO (1925–1942), (2) −PDO and +AMO (1945–1959 and 2001–2016), (3) +PDO and −AMO (1980–1995), and (4) −PDO and −AMO (1910–1924 and 1960–1979).

4. Composites of summer rainfall and monsoon under varying AMO and PDO phases

To reveal the synergistic impacts of the PDO and AMO on summer rainfall (hereafter we discuss only the rainfall anomalies in summertime) over Northeast Asia, composite rainfall anomalies are constructed for the aforementioned four combinations of the PDO and AMO phases (Fig. 3). In the case of +AMO, excessive rainfall occurs over the upper reaches of the Huaihe River, the middle reaches of the Yellow River, Northeast China, and the Korean Peninsula, while the rainfall over the Bohai–to–Yellow Sea bay rim regions (lower reaches of the Huaihe River and Yellow River, southern part of Northeast China and the Korean Peninsula) is deficient during +PDO (Fig. 3a) but excessive during −PDO (Fig. 3b). During +PDO, deficient rainfall occurs over most parts of the Bohai–to–Yellow Sea bay rim regions, whereas the rainfall over the upper reaches of the Huaihe River, the middle reaches of the Yellow River, Northeast China and the northern Korean Peninsula is excessive during +AMO (Fig. 3a) but deficient during −AMO (Fig. 3c). Among the four categories, deficient rainfall covers nearly all parts of Northeast Asia during −AMO and +PDO, while the rainfall becomes excessive during +AMO and −PDO.

Under −AMO/−PDO, the anomalous rainfall pattern is more reminiscent of the drought in the first half of the mid-1960s–1990s, with less rainfall in the Huaihe River valley, the middle reaches of the Yellow River, and the Korean Peninsula (Fig. 3d). With −AMO and +PDO, the pattern is more reminiscent of the drought in the second half of the 1960s–1990s, and less rainfall occurs in nearly all parts of Northeast Asia (Fig. 3c). As seen in Fig. 4, the region with the highest summer rainfall in Northeast Asia associated with the AMO is situated in the upper reaches of the Huaihe River, the middle reaches of the Yellow River, Northeast China, and the Korean Peninsula. The region with the lowest rainfall associated with the PDO encompasses the Bohai–to–Yel-

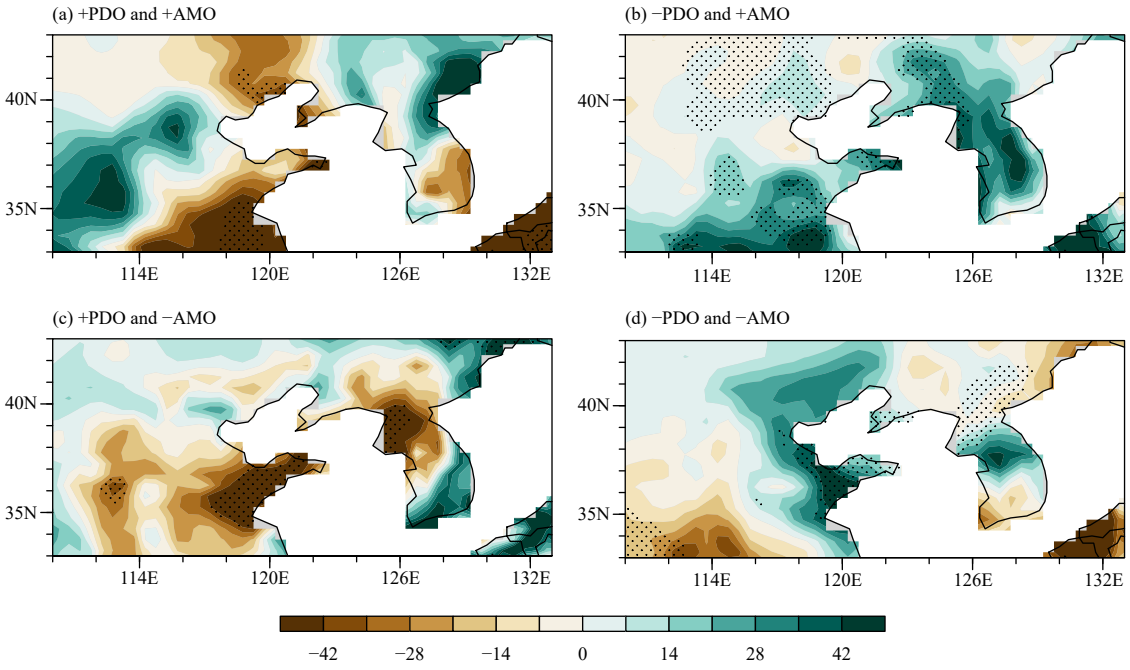

Fig. 3. Composite summer rainfall anomalies (mm) (relative to the 1901–2016 mean) from the CRU dataset for the four regimes: (a) positive phase PDO and positive phase AMO, (b) negative phase PDO and positive phase AMO, (c) positive phase PDO and negative phase AMO, and (d) negative phase PDO and negative phase AMO. Values exceeding the 95% confidence level are stippled.

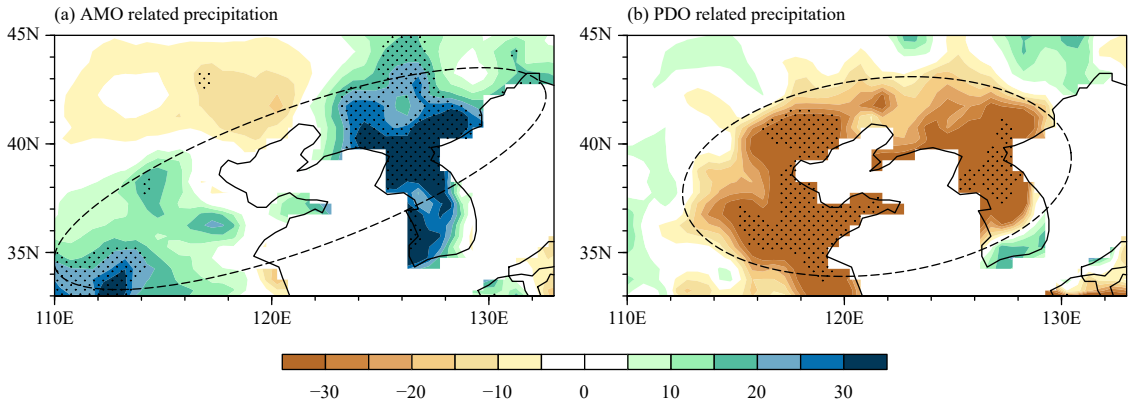

Fig. 4. Regression of the summer rainfall (mm) from the CRU dataset on the (a) AMO and (b) PDO indices. Values exceeding the 95% confidence level are stippled.

low Sea bay rim regions. These results suggest that the AMO and PDO are two key factors affecting the interdecadal variation of summer rainfall over Northeast Asia, and their impacts are generally complementary.

To address the atmospheric processes through which the AMO and PDO jointly affect the interdecadal change of summer precipitation over Northeast Asia, we first examine their individual impacts. The geopotential height pattern associated with the AMO indicates a distinct circumglobal wave train in the Northern Hemisphere (Si and Ding, 2016), with seven centers of action extending from the North Atlantic through continental Eurasia to the North Pacific (hereafter the ANH pattern). In the North Atlantic sector, a southwest–northeast-tilted "high–low–high" type pattern is closely linked to the decadal climate change in Europe, such as the anomalously dry summers in northern Europe and wet summers in southern Europe during the 1960s–1980s (Sutton and Hodson, 2005) and the opposite trend in the 1990s (Sutton and Dong, 2012). An enhanced (weakened) warming associated with a positive (negative) phase of the AMO induces an eastward propagation of midlatitude Rossby waves across continental Eurasia (Sun et al., 2015; Zhao et al., 2020). Corresponding to +AMO, a zonal tripole pattern is located in the Northeast Asia–North Pacific sector, with two centers of high pressure over central Siberia and the midlatitude western North Pacific, and a low over Northeast Asia (Fig. 5a). The anomalous geopotential height pattern indicates that the AMO could induce this tripole pattern through the ANH teleconnection. For instance, a warm North Atlantic (+AMO) may contribute to the occurrence of two centers of high pressure over central Siberia and the midlatitude western North Pacific Ocean, and a cold vortex over Northeast Asia in summer. Idealized numerical experiments suggest that +AMO can enhance the high pressure over Siberia through a quasi-stationary Rossby wave train (Sun et al., 2015). The high pressure over Siberia is favorable for southward intrusion of cold air from the Arctic and high latitudes to Northeast Asia. In the lower troposphere, the zonal tripolar pattern corresponds to an anomalous cyclone in Northeast Asia and an anomalous anticyclone in

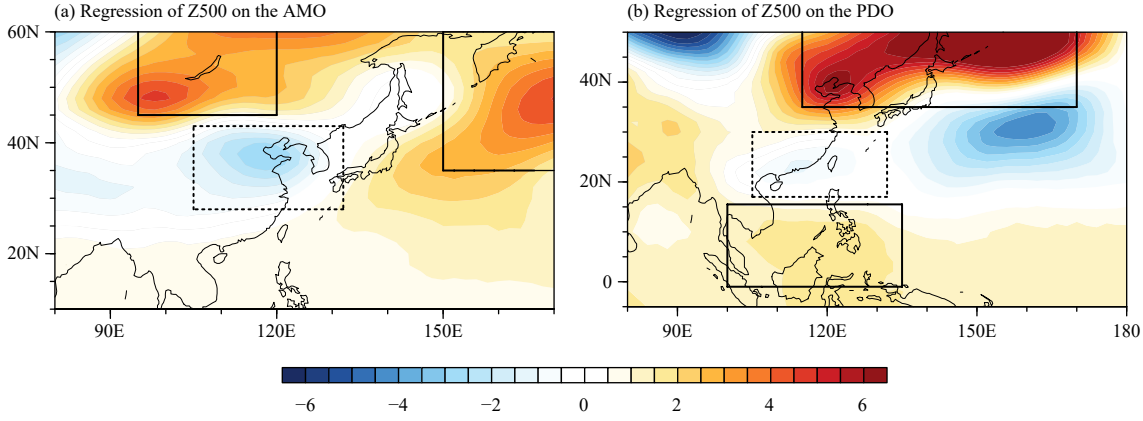

Fig. 5. Regression of the 500-hPa geopotential height (Z500; gpm) in summer on the (a) AMO and (b) PDO indices. The solid and dashed outlines denote anomalous high and low geopotential heights, respectively.

Siberia (Fig. 6a). The strong Siberian anticyclone conveys the cold air from the high latitudes southward to Northeast Asia. Meanwhile, a strong East Asian summer monsoon corresponds to strong southwesterly wind dominating over central and southern East Asia, which transports humid and warm air northward to Northeast Asia. The northward warm air mass converges with the southward cold air mass over Northeast Asia, which leads to above-normal summer rainfall over the region (Fig. 4a).

Regression of the geopotential height pattern on the PDO index indicates that a meridional tripole-type wave train extends from the western tropical Pacific through Northeast Asia to the mid-North Pacific (Fig. 5b), which resembles the East Asia–Pacific/Pacific–Japan (EAP/PJ) teleconnection (Nitta, 1987; Huang and Li, 1988). The EAP/PJ teleconnection is believed to be related to the northeastward propagation of Rossby waves, which is linked to, and likely originates from, the tropical Northwest Pacific Ocean (Nitta, 1987). The Rossby waves are excited by the anomalous convective heating in the tropical Northwest Pacific, which is strongly modulated by the SST anomalies in the tropical Northwest Pacific associated with the PDO. A +PDO corresponds to cold SSTs over the tropical western Pacific and warm SSTs over the tropical central and eastern Pacific (Mantua et al., 1997). The weakened convection over the tropical Northwest Pacific, attributable to cold SSTs, generates a "high–low–high" EAP/PJ pattern. In the lower troposphere, an anomalous anticyclone locates over the tropical Northwest Pacific and Northeast Asia, while an anomalous cyclone locates over the southeast coast of China (Fig. 6b). This anomalous circulation pattern weakens the East Asian summer monsoon and the water vapor transport from the tropics to the mid and high latitudes, and in turn decreases summer rainfall over Northeast Asia (Fig. 4b).

The composite large-scale anomalous atmospheric circulation patterns under the four categories of the PDO and AMO phases are shown in Fig. 7. In the case of +AMO, the ANH pattern contributes to a "high–low–high" like zonal anomalous pattern over the Northeast Asia–North Pacific sector, while the geopotential height anomalies over the southeast coast of China are negative during +PDO (Fig. 7a) but positive during −PDO (Fig. 7b). In the case of +AMO, a zonal anticyclone–cyclone–anticyclone wave train extends in the lower troposphere from Siberia to the midlatitude western North Pacific. The anomalous circulation over the southeast coast of China is cyclonic and the East Asian summer monsoon is weak during +PDO (Fig. 8a), whereas the opposite holds during −PDO (Fig. 8b). The −PDO enhances the East Asian summer monsoon and the cyclonic anomalies over Northeast Asia via the EAP/PJ teleconnection pattern (Fig. 8b), leading to more rainfall in Northeast Asia (Fig. 3b). In contrast, the +PDO weakens the East Asian summer monsoon and the cyclonic anomalies over Northeast Asia via the EAP/PJ pattern, and the water vapor convergence is stronger over the upper reaches of the Huaihe River, the middle reaches of the Yellow River, Northeast China, and the northern Korean Peninsula, but weaker over the Bohai–to–Yellow Sea bay rim regions (Fig. 8a), which results in an anomalous rainfall pattern consistent with that shown in Fig. 3a.

Under −AMO, the ANH shifts to an opposite sign to that under +AMO, with the geopotential height anomalies over the southeast coast of China turning negative during +PDO (Fig. 7c) but positive during −PDO (Fig. 7d). In the lower troposphere, under −AMO, anticyclonic anomalies emerge over Northeast Asia, the circulation over the southeast coast of China is cyclonic, and the East Asian summer monsoon is weak during +PDO (Fig.

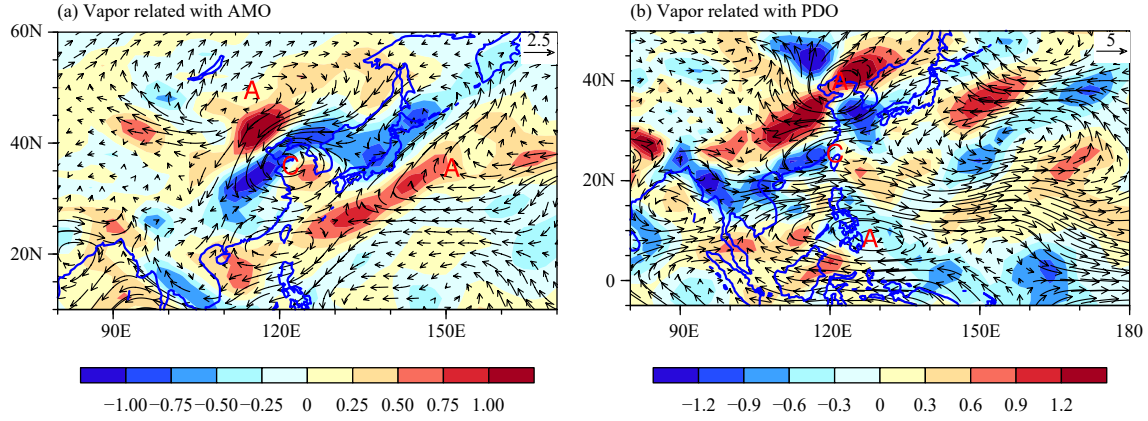

Fig. 6. Regression of the 850-hPa moisture flux (vector; kg s^{-1} m^{-1}) and divergence (shading; 10^{-6} kg s^{-1} m^{-2}) fields on the (a) AMO and (b) PDO indices. The letters C and A denote an anomalous cyclone and anticyclone, respectively.

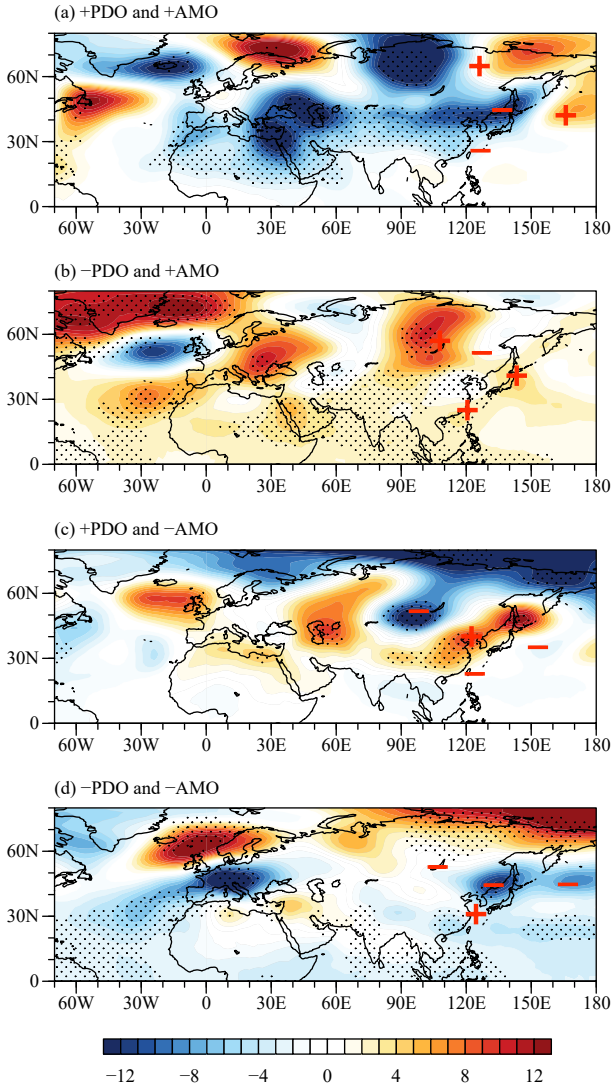

Fig. 7. As in Fig. 3, but for the anomalous 500-hPa geopotential height (gpm) pattern. The symbols + and − denote anomalous high and low geopotential heights, respectively.

8c). Conversely, the circulation over the southeast coast of China is anticyclonic and the East Asian summer monsoon is strong during −PDO (Fig. 8d).

The −PDO enhances the East Asian summer monsoon and weakens the anticyclonic anomalies over Northeast Asia via the EAP/PJ teleconnection pattern (Fig. 8d), thus leading to moderately excessive rainfall over Northeast Asia (Fig. 3d). In contrast, +PDO weakens the East Asian summer monsoon and enhances the anticyclonic anomalies over Northeast Asia via the EAP/PJ pattern. The water vapor divergence is enhanced over Northeast Asia (Fig. 8c), which results in remarkably deficient rainfall over Northeast Asia (Fig. 3c).

The above results indicate that the interdecadal change of Northeast Asian summer rainfall is strongly modulated by the AMO and PDO. With +AMO and −PDO, an anomalous cyclone dominates Northeast Asia and the East Asian summer monsoon is strong, and rainfall over the whole region is excessive, which is more reminiscent of the mid-1940s to early 1960s pluvial period. With −AMO and +PDO, the rainfall and atmospheric circulation anomalies become roughly opposite in sign, and the rainfall over the whole region is deficient, which is more reminiscent of the drought in the second half of the 1960s–1990s. With −AMO and −PDO, the East Asian summer monsoon is slightly stronger than normal, and a small anomalous cyclone situates over the Bohai–to–Yellow Sea bay rim regions. These anomalies lead to more rainfall over the coastal rim areas but less over the rest of the region, which is more reminiscent of the drought in the first half of the mid-1960s–1990s. With +AMO and +PDO, the East Asian summer monsoon is weak, and a large anomalous cyclone with a weak center situates in Northeast Asia, resulting in less rainfall over the coastal rim regions but more over the remaining regions.

5. Modeling results

We also examine the synergistic impacts of the PDO and AMO on Northeast Asian summer rainfall in the CESM-LE large ensemble historical simulations. Among the 40 members of the CESM-LE, member-7 has the best skill in simulating the observed PDO and AMO indices. The correlation coefficients of the PDO and AMO indices between the observation and member-7 are 0.41 and 0.65, respectively. Using the AMO and PDO indices simulated by member-7, we first identify the positive and negative phases of the AMO and PDO in the CESM-LE simulations (Fig. 9). Similar to the observational data, they are grouped into four general categories: (1) +PDO and +AMO, (2) −PDO and +AMO, (3) +PDO and −AMO, and (4) −PDO and −AMO. The composites of the SST and rainfall anomalies are then constructed.

Under +AMO and +PDO, warm SSTs appear in the North Atlantic and the tropical eastern and central Pacific but cold SSTs in the midlatitude North Pacific (Fig. 10a), while the opposite pattern holds under −AMO and −PDO (Fig. 10d). With −AMO and +PDO, cold SSTs occur in the North Atlantic and midlatitude North Pacific but warm SSTs in the tropical eastern and central Pacific (Fig. 10c), and the opposite trends are true during +AMO and −PDO (Fig. 10b). Member-7 of CESM-LE reproduces well the positive correlation between the AMO and Northeast Asian summer rainfall (Fig. 11). Compared with the observations, the high-correlation regions in East China shift slightly southward to the south of the

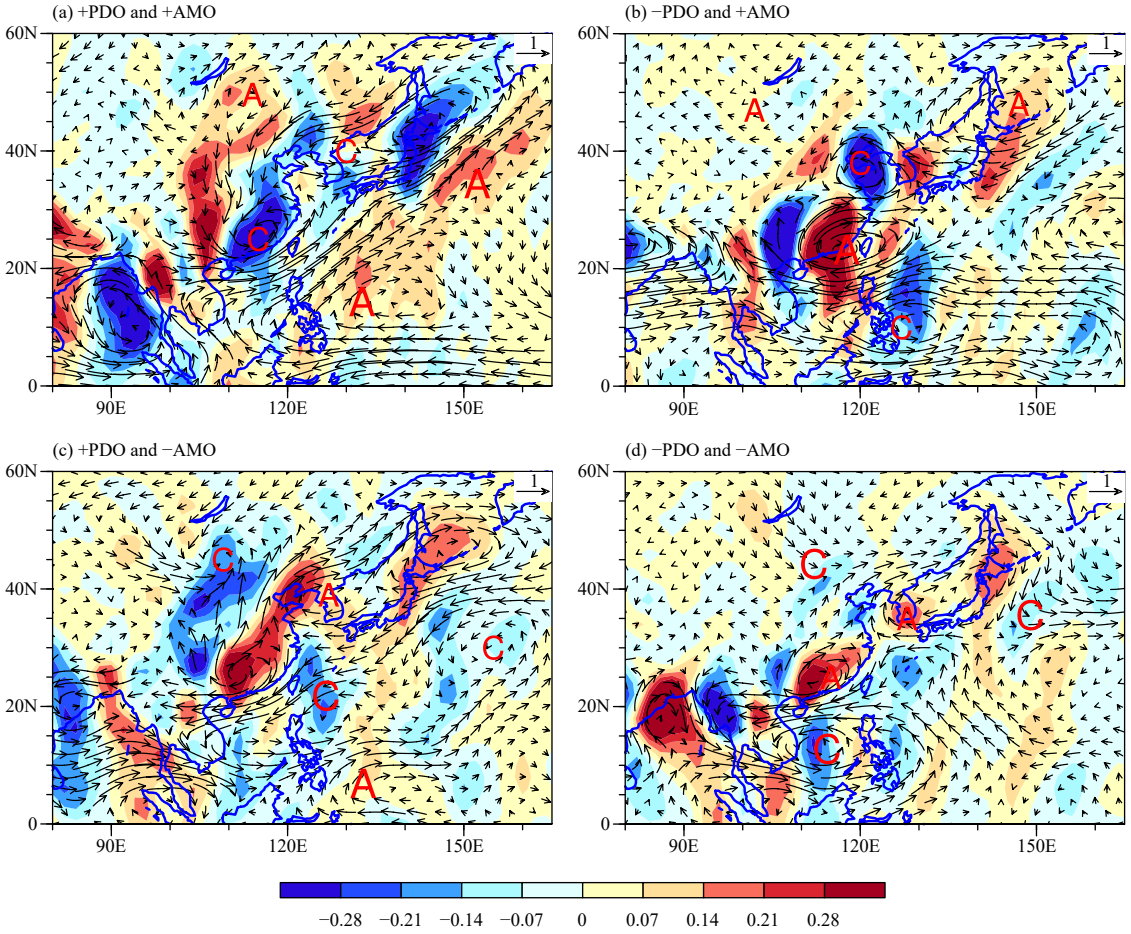

Fig. 8. As in Fig. 3, but for the 850-hPa moisture flux (vectors; kg s^{-1} m^{-1}) anomalies and the divergence field (shading; 10^{-6} kg s^{-1} m^{-2}). The letters C and A denote an anomalous cyclone and anticyclone, respectively.

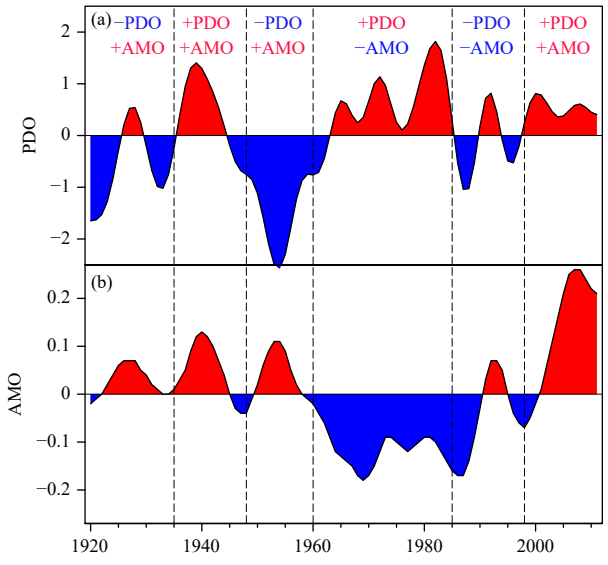

Fig. 9. As in Fig. 1, but for the simulations by member-7 of the Community Earth System Model large ensemble (CESM-LE).

Yellow River. The model also captures the negative correlation between the PDO and summer rainfall over Northeast Asia, and the high-correlation regions shift more northward compared to the observation and are situated in Northeast China. Thus, the high summer rainfall regions over Northeast Asia related with the AMO are mainly located in the southern part of Northeast Asia, while those related to the PDO are mainly in the northern part in the CESM-LE simulations.

Member-7 of the CESM-LE simulates well the excessive summer rainfall over the whole region under the −PDO and +AMO category (Fig. 12), with the maximum anomalies emerging in Northeast China and the Huaihe River valley. Meanwhile, the rainfall over the Yellow River valley and Korean Peninsula is slightly deficient. The model generally reproduces the deficit over the whole region under the +PDO and −AMO category, but the rainfall over the Korean Peninsula and parts of the Yellow River valley is moderately excessive. Additionally, under the +PDO and +AMO category, the anomalous rainfall over Northeast Asia in the simulations follows a "north less and south more" pattern, and the opposite holds under −PDO and −AMO. While the model

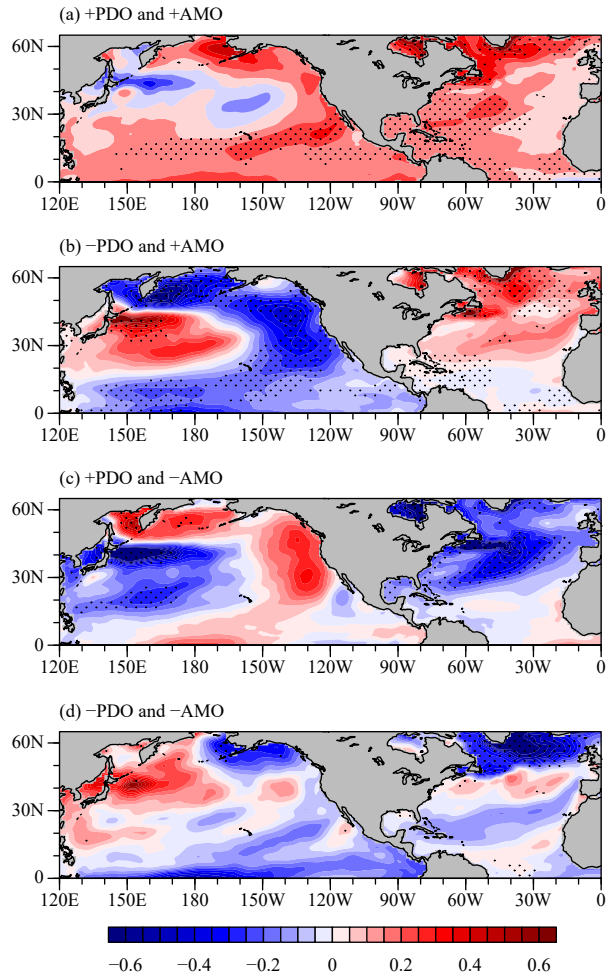

Fig. 10. Composite detrended SST (K) anomalies for the four regimes simulated by member-7 of the CESM-LE: (a) positive phase PDO and positive phase AMO, (b) negative phase PDO and positive phase AMO, (c) positive phase PDO and negative phase AMO, and (d) negative phase PDO and negative phase AMO. Values exceeding the 95% confidence level are stippled.

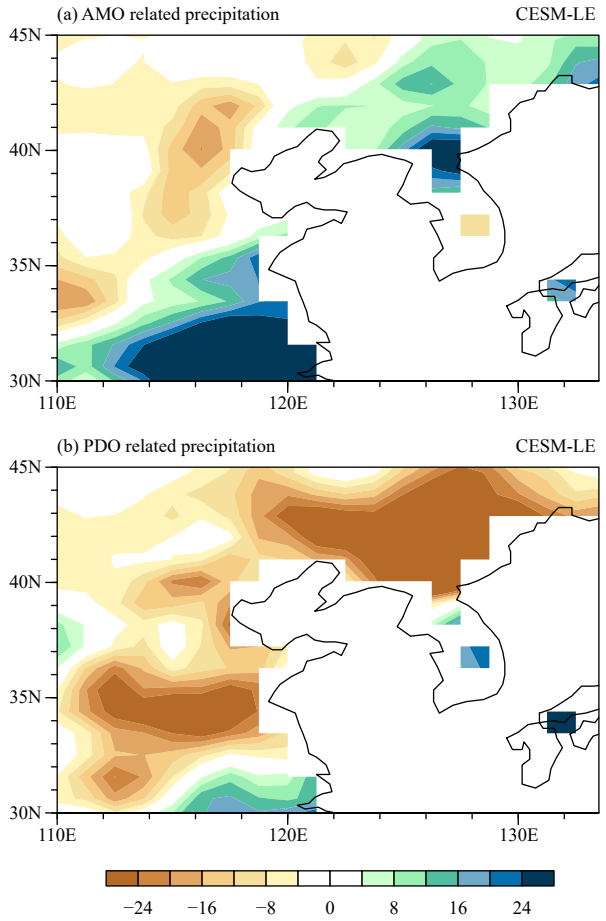

Fig. 11. Regression of the summer rainfall (mm) on the (a) AMO and (b) PDO indices simulated by member-7 of the CESM-LE.

fails to reproduce the regional rainfall anomalies in the Huaihe River valley and southern Korea under the +PDO and +AMO and the −PDO and −AMO categories. As seen in Figs. 12a, d, the simulated rainfall anomalies in these regions are opposite to those in the observation (Figs. 3a, d).

The above analysis reveals that CESM-LE generally reproduces the synergistic impacts of AMO and PDO on the summer rainfall in Northeast Asia. These observational and modeling results confirm that the AMO and PDO are the two key factors affecting the interdecadal change of Northeast Asian summer climate.

6. Summary and discussion

This study has comprehensively investigated the synergistic impacts of the AMO and PDO on the interdecadal change of summer rainfall over Northeast Asia based on both observations and simulations. The conclusions can be summarized as follows.

(1) The AMO and PDO are the two major factors jointly affecting the interdecadal change of summer rainfall over Northeast Asia. The PDO-related summer rainfall anomaly mainly occurs in the Bohai–to–Yellow Sea bay rim regions, while the AMO-related one locates over the rest of Northeast Asia.

(2) The AMO induces a zonal tripole pattern from Lake Baikal to the western North Pacific via a circumglobal teleconnection wave train. Under +AMO (−AMO), high pressure (low pressure) exists over Siberia and the western North Pacific, and low pressure (high pressure) exists over Northeast Asia, which leads to a strong (weak) East Asian summer monsoon and more (less) summer rainfall in Northeast Asia. The PDO modulates the summer monsoon over East Asia and rainfall over Northeast Asia via the EAP/PJ meridional teleconnection pattern. A +PDO (−PDO) results in less (more) summer rainfall over Northeast Asia and a weak (strong) East

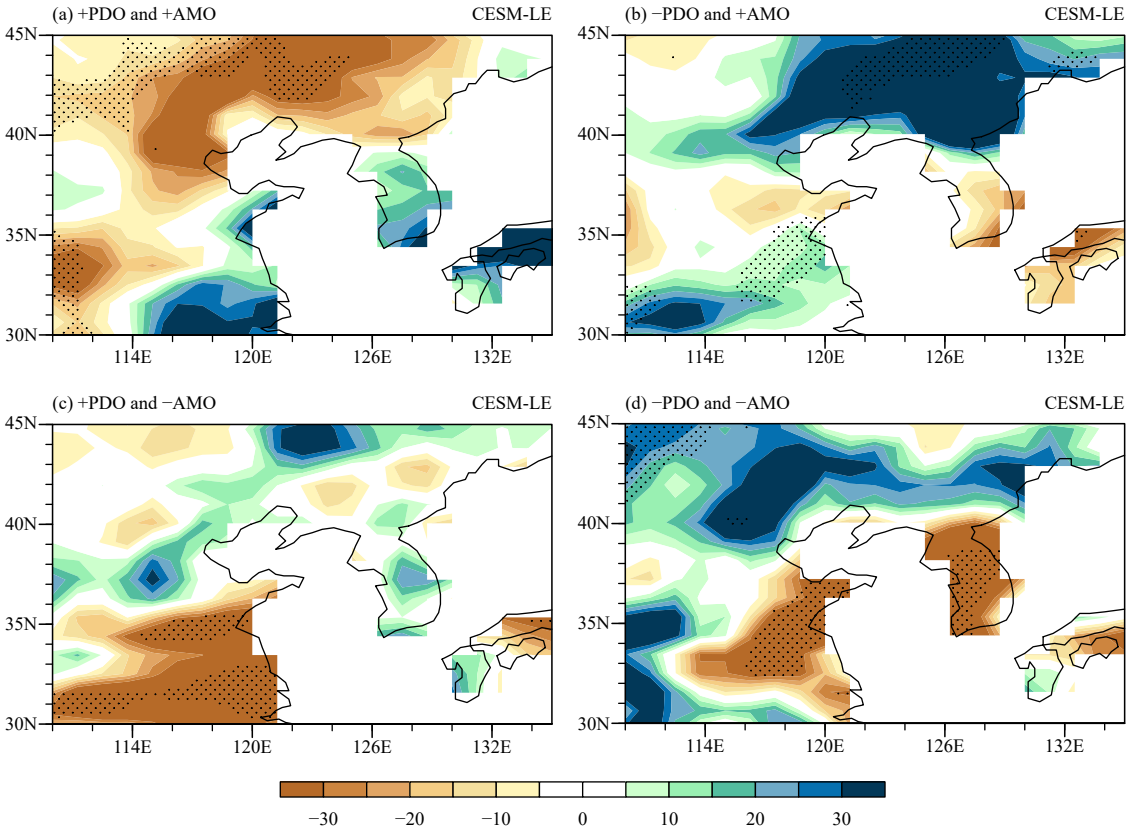

Fig. 12. As in Fig. 3, but for the simulations by member-7 of the CESM-LE.

Asian summer monsoon.

(3) The proposed mechanisms for the synergistic impacts of the AMO and PDO on the interdecadal change of summer rainfall over Northeast Asia are presented in Fig. 13. Under +AMO and −PDO, an anomalous cyclone dominates Northeast Asia, and the East Asian summer monsoon is strong, resulting in excessive rainfall over the whole region. This situation is more reminiscent of the mid-1940s–early 1960s pluvial period. When the phases of the AMO and PDO are reversed, i.e., −AMO and +PDO, Northeast Asia receives deficient rainfall, and East Asia experiences a weak summer monsoon, which is more reminiscent of the drought in the second half of the 1960s–1990s.

Under −AMO and −PDO, the East Asian summer monsoon is slightly stronger than normal and a small anomalous cyclone situates over the Bohai–to–Yellow Sea bay rim regions. These result in excessive rainfall over the coastal rim areas and deficient rainfall over the rest of the region, which is more reminiscent of the drought in the first half of the mid-1960s–1990s. When the phases of the AMO and PDO are reversed, i.e., +AMO and +PDO, the East Asian summer monsoon is slightly weak, and a large anomalous cyclone with a weak center situates over Northeast Asia. This results in the coastal rim areas experiencing deficient rainfall, whereas the rest of the region receives excessive rainfall.

This study reveals that both the AMO and PDO strongly affect the interdecadal climate of Northeast Asia, with the AMO acting through a zonal midlatitude way and the PDO through a meridional tropical–midlatitude way. The change of the East Asian summer monsoon and Northeast Asia rainfall differs considerably under different combinations of the AMO and PDO phases. The most direct and impactful atmospheric circulation on Northeast Asian summer rainfall is the local or regional cyclonic or anticyclonic circulation system, which is modulated by both the AMO and PDO. Compared with the PDO, the AMO plays a more significant role in altering the regional atmospheric circulation in Northeast Asia. However, the PDO exerts a more important role in modulating the large-scale atmospheric circulation and summer rainfall over the low and midlatitudes of East Asia and the western North Pacific through the EAP/PJ pattern.

The drought in the mid-1960s–1990s began under a −AMO and −PDO situation in the mid-1960s, then increased in severity under a −AMO and +PDO situation in

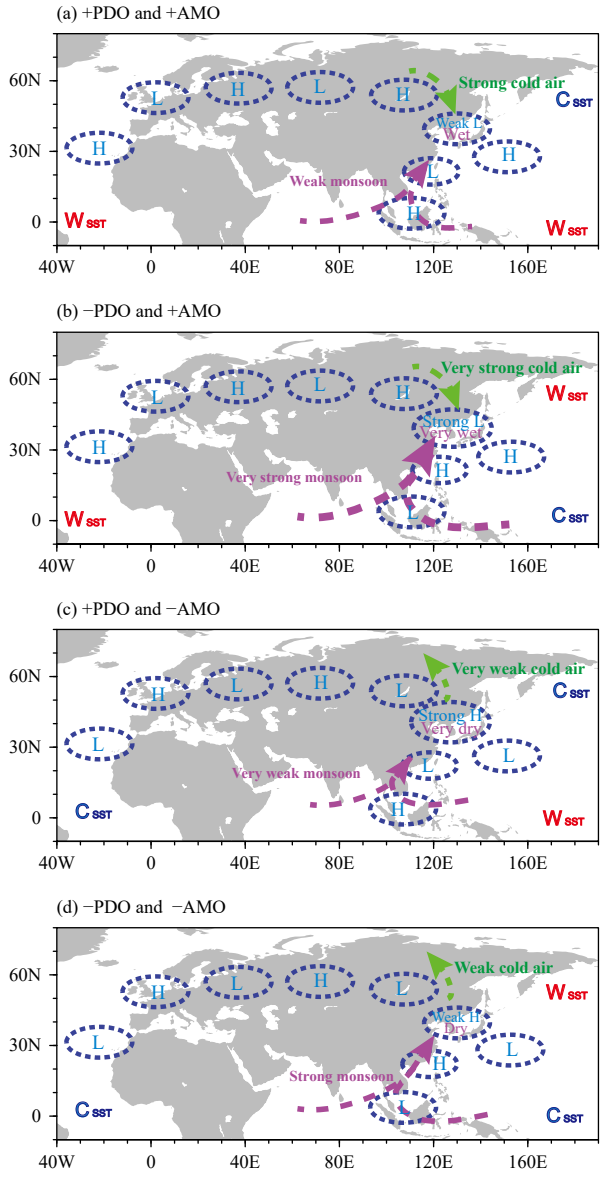

Fig. 13. Schematic diagram of the synergistic impacts of the PDO and AMO on the summer rainfall over Northeast Asia. The red W and blue C indicate warm and cold SSTs, respectively. The letters H and L indicate high and low geopotential heights, respectively. The green curves with arrows denote the cold flow. The purple curves with arrows indicate the monsoon flow.

the 1980s, and finally ended under a +AMO and −PDO situation in the late 1990s. Previous studies have shown that the East Asian rain belt has shifted northward from south of the Yangtze River valley to north of the Yangtze River valley (Si et al., 2009; Huang et al., 2011; Si and Ding, 2013; Ding et al., 2020), which has mitigated drought conditions in the middle and lower reaches of the Yellow and Huaihe Rivers. The synergistic impacts of the AMO and PDO not only exert a significant influence on the Northeast Asian summer climate, but also add complexity in understanding and predicting low-frequency climate variability in Northeast Asia due to the decadal to multidecadal modulation produced by the AMO and PDO.

Acknowledgments. The authors would like to thank the Editor and two anonymous reviewers, whose critical and constructive comments significantly improve this paper. We acknowledge the CESM Large Ensemble Project.

REFERENCES

Bueh, C., Y. Li, D. W. Lin, et al., 2016: Interannual variability of summer rainfall over the northern part of China and the related circulation features. *J. Meteor. Res.*, **30**, 615–630, doi: 10.1007/s13351-016-5111-5.

Compo, G. P., J. S. Whitaker, P. D. Sardeshmukh, et al., 2011: The twentieth century reanalysis project. *Quart. J. Roy. Meteor. Soc.*, **137**, 1–28, doi: 10.1002/qj.776.

Ding, Y. H., Y. Sun, Z. Y. Wang, et al., 2009: Inter-decadal variation of the summer precipitation in China and its association with decreasing Asian summer monsoon Part II: Possible causes. *Int. J. Climatol.*, **29**, 1926–1944, doi: 10.1002/joc.1759.

Ding, Y. H., P. Liang, Y. J. Liu, et al., 2020: Multiscale variability of Meiyu and its prediction: A new review. *J. Geophys. Res. Atmos.*, **125**, e2019JD031496, doi: 10.1029/2019JD031496.

Fan, Y., K. Fan, X. H. Zhu, et al., 2019: El Niño-related summer precipitation anomalies in Southeast Asia modulated by the Atlantic multidecadal oscillation. *J. Climate*, **32**, 7971–7987, doi: 10.1175/JCLI-D-19-0049.1.

Gao, Z. T., Z. Z. Hu, B. Jha, et al., 2014: Variability and predictability of Northeast China climate during 1948–2012. *Climate Dyn.*, **43**, 787–804, doi: 10.1007/s00382-013-1944-0.

Gong, Z. Q., S. F. Li, P. Hu, et al., 2016: Dynamic–analogue correction of the decadal change of East Asian summer precipitation in the late 1990s. *J. Meteor. Res.*, **30**, 341–355, doi: 10.1007/s13351-016-5220-1.

Ha, K. J., B. H. Kim, E. S. Chung, et al., 2020: Major factors of global and regional monsoon rainfall changes: Natural versus anthropogenic forcing. *Environ. Res. Lett.*, **15**, 034055, doi: 10.1088/1748-9326/ab7767.

Hu, Z. Y., A. X. Hu, and Y. Y. Hu, 2018: Contributions of interdecadal Pacific oscillation and Atlantic multidecadal oscillation to global ocean heat content distribution. *J. Climate*, **31**, 1227–1244, doi: 10.1175/JCLI-D-17-0204.1.

Huang, D. Q., J. Zhu, and X. Y. Kuang, 2011: Decadal variation of different durations of continuous Meiyu precipitation and the possible cause. *Chinese Sci. Bull.*, **56**, 424–431, doi: 10.1007/s11434-010-4241-x.

Huang, R. H., and W. J. Li, 1988: Influence of heat source anomaly over the western tropical Pacific on the subtropical high over East Asia and its physical mechanism. *Chinese J. Atmos. Sci.*, **12**, 107–116, doi: 10.3878/j.issn.1006-9895.1988.t1.08. (in Chinese)

Hurrell, J. W., J. J. Hack, D. Shea, et al., 2008: A new sea surface temperature and sea ice boundary dataset for the Community Atmosphere Model. *J. Climate*, **21**, 5145–5153, doi: 10.1175/2008JCLI2292.1.

Hurrell, J. W., M. M. Holland, P. R. Gent, et al., 2013: The Com-

munity Earth System Model: A framework for collaborative research. *Bull. Amer. Meteor. Soc.*, **94**, 1339–1360, doi: 10.1175/BAMS-D-12-00121.1.

Jiang, D. B., and H. J. Wang, 2005: Natural interdecadal weakening of East Asian summer monsoon in the late 20th century. *Chinese Sci. Bull.*, **50**, 1923–1929, doi: 10.1360/982005-36.

Jiang, D. B., D. Si, and X. M. Lang, 2020: Evaluation of East Asian summer climate prediction from the CESM large-ensemble initialized decadal prediction project. *J. Meteor. Res.*, **34**, 252–263, doi: 10.1007/s13351-020-9151-5.

Kay, J. E., C. Deser, A. Phillips, et al., 2015: The Community Earth System Model (CESM) large ensemble project: A community resource for studying climate change in the presence of internal climate variability. *Bull. Amer. Meteor. Soc.*, **96**, 1333–1349, doi: 10.1175/BAMS-D-13-00255.1.

Kim, D. W., H. R. Byun, K. S. Choi, et al., 2011: A spatiotemporal analysis of historical droughts in Korea. *J. Appl. Meteor. Climatol.*, **50**, 1895–1912, doi: 10.1175/2011JAMC2664.1.

Lee, E. J., J. G. Jhun, and C. K. Park, 2005: Remote connection of the Northeast Asian summer rainfall variation revealed by a newly defined monsoon index. *J. Climate*, **18**, 4381–4393, doi: 10.1175/JCLI3545.1.

Li, Y., Y. H. Ding, and W. J. Li, 2017: Interdecadal variability of the Afro-Asian summer monsoon system. *Adv. Atmos. Sci.*, **34**, 833–846, doi: 10.1007/s00376-017-6247-7.

Liu, H. B., M. Wen, J. H. He, et al., 2012: Characteristics of the Northeast cold vortex at intraseasonal time scale and its impact. *Chinese J. Atmos. Sci.*, **36**, 959–973, doi: 10.3878/j.issn.1006-9895.2012.11167. (in Chinese)

Liu, S., S. Yang, Y. Lian, et al., 2010: Time–frequency characteristics of regional climate over Northeast China and their relationships with atmospheric circulation patterns. *J. Climate*, **23**, 4956–4972, doi: 10.1175/2010JCLI3554.1.

Liu, Y., W. Zhou, X. Qu, et al., 2020: An interdecadal change of the boreal summer Silk Road pattern around the late 1990s. *J. Climate*, **33**, 7083–7100, doi: 10.1175/JCLI-D-19-0795.1.

Lu, M. M., B. H. Huang, Z. N. Li, et al., 2019: Role of Atlantic air–sea interaction in modulating the effect of Tibetan Plateau heating on the upstream climate over Afro-Eurasia–Atlantic regions. *Climate Dyn.*, **53**, 509–519, doi: 10.1007/s00382-018-4595-3.

Lu, R. Y., B. W. Dong, and H. Ding, 2006: Impact of the Atlantic Multidecadal Oscillation on the Asian summer monsoon. *Geophys. Res. Lett.*, **33**, L24701, doi: 10.1029/2006GL027655.

Luo, F. F., S. L. Li, and T. Furevik, 2011: The connection between the Atlantic Multidecadal Oscillation and the Indian Summer Monsoon in Bergen Climate Model Version 2.0. *J. Geophys. Res. Atmos.*, **116**, D19117, doi: 10.1029/2011JD015848.

Ma, Z. G., 2007: The interdecadal trend and shift of dry/wet over the central part of North China and their relationship to the Pacific Decadal Oscillation (PDO). *Chinese Sci. Bull.*, **52**, 2130–2139, doi: 10.1007/s11434-007-0284-z.

Ma, Z. G., and C. B. Fu, 2006: Some evidence of drying trend over northern China from 1951 to 2004. *Chinese Sci. Bull.*, **51**, 2913–2925, doi: 10.1007/s11434-006-2159-0.

Mantua, N. J., S. R. Hare, Y. Zhang, et al., 1997: A Pacific interdecadal climate oscillation with impacts on salmon production. *Bull. Amer. Meteor. Soc.*, **78**, 1069–1080, doi: 10.1175/1520-0477(1997)078<1069:APICOW>2.0.CO;2.

Nath, R., and Y. Luo, 2019: Disentangling the influencing factors driving the cooling trend in boreal summer over Indo-Gangetic river basin, India: role of Atlantic multidecadal oscillation (AMO). *Theor. Appl. Climatol.*, **138**, 1–12, doi: 10.1007/s00704-019-02779-y.

Nitta, T., 1987: Convective activities in the tropical western Pacific and their impact on the Northern Hemisphere summer circulation. *J. Meteor. Soc. Japan*, **65**, 373–390, doi: 10.2151/jmsj1965.65.3_373.

Piao, J. L., W. Chen, and S. F. Chen, 2021: Water vapour transport changes associated with the interdecadal decrease in the summer rainfall over Northeast Asia around the late-1990s. *Int. J. Climatol.*, **41**, E1469–E1482, doi: 10.1002/joc.6780.

Qian, C., and T. J. Zhou, 2014: Multidecadal variability of North China aridity and its relationship to PDO during 1900–2010. *J. Climate*, **27**, 1210–1222, doi: 10.1175/JCLI-D-13-00235.1.

Qin, M. H., D. L. Li, A. G. Dai, et al., 2018: The influence of the Pacific Decadal Oscillation on North Central China precipitation during boreal autumn. *Int. J. Climatol.*, **38**, e821–e831, doi: 10.1002/joc.5410.

Schlesinger, M. E., and N. Ramankutty, 1994: An oscillation in the global climate system of period 65–70 years. *Nature*, **367**, 723–726, doi: 10.1038/367723a0.

Si, D., and Y. H. Ding, 2013: Decadal change in the correlation pattern between the Tibetan Plateau winter snow and the East Asian summer precipitation during 1979–2011. *J. Climate*, **26**, 7622–7634, doi: 10.1175/JCLI-D-12-00587.1.

Si, D., and Y. H. Ding, 2016: Oceanic forcings of the interdecadal variability in East Asian summer rainfall. *J. Climate*, **29**, 7633–7649, doi: 10.1175/JCLI-D-15-0792.1.

Si, D., Y. H. Ding, and Y. J. Liu, 2009: Decadal northward shift of the Meiyu belt and the possible cause. *Chinese Sci. Bull.*, **54**, 4742–4748, doi: 10.1007/s11434-009-0385-y.

Si, D., D. B. Jiang, A. X. Hu, et al., 2021: Variations in Northeast Asian summer precipitation driven by the Atlantic multidecadal oscillation. *Int. J. Climatol.*, **41**, 1682–1695, doi: 10.1002/joc.6912.

Sun, C., J. P. Li, and S. Zhao, 2015: Remote influence of Atlantic multidecadal variability on Siberian warm season precipitation. *Sci. Rep.*, **5**, 16853, doi: 10.1038/srep16853.

Sutton, R. T., and D. L. R. Hodson, 2005: Atlantic Ocean forcing of North American and European summer climate. *Science*, **309**, 115–118, doi: 10.1126/science.1109496.

Sutton, R. T., and B. W. Dong, 2012: Atlantic Ocean influence on a shift in European climate in the 1990s. *Nat. Geosci.*, **5**, 788–792, doi: 10.1038/ngeo1595.

Ting, M., Y. Kushnir, R. Seager, et al., 2011: Robust features of Atlantic multi-decadal variability and its climate impacts. *Geophys. Res. Lett.*, **38**, L17705, doi: 10.1029/2011GL048712.

Wang, H., S. P. Xie, Y. Kosaka, et al., 2019: Dynamics of Asian summer monsoon response to anthropogenic aerosol forcing. *J. Climate*, **32**, 843–858, doi: 10.1175/JCLI-D-18-0386.1.

Wang, S. W., D. Y. Gong, J. L. Ye, et al., 2000: Seasonal precipitation series of eastern China since 1880 and the variability. *Acta Geogr. Sinica*, **55**, 281–293, doi: 10.3321/j.issn:0375-5444.2000.03.004. (in Chinese)

Wu, B., T. J. Zhou, and T. Li, 2016: Impacts of the Pacific–Japan and circumglobal teleconnection patterns on the interdecadal

variability of the East Asian summer monsoon. *J. Climate*, **29**, 3253–3271, doi: 10.1175/JCLI-D-15-0105.1.

Xie, Z. W., and C. Bueh, 2017: Cold vortex events over Northeast China associated with the Yakutsk–Okhotsk blocking. *Int. J. Climatol.*, **37**, 381–398, doi: 10.1002/joc.4711.

Yan, X., J. Z. Ren, J. H. Ju, et al., 2018: Influence of springtime Atlantic SST on ENSO: Role of the Madden–Julian Oscillation. *J. Meteor. Res.*, **32**, 380–393, doi: 10.1007/s13351-018-7046-5.

Zhang, Z. Q., X. G. Sun, and X. Q. Yang, 2018: Understanding the interdecadal variability of East Asian summer monsoon precipitation: Joint influence of three oceanic signals. *J. Climate*, **31**, 5485–5506, doi: 10.1175/JCLI-D-17-0657.1.

Zhao, W., W. Chen, S. F. Chen, et al., 2020: Interdecadal change in the impact of North Atlantic SST on August rainfall over the monsoon transitional belt in China around the late 1990s. *Theor. Appl. Climatol.*, **140**, 503–516, doi: 10.1007/s00704-020-03102-w.

Zheng, J. Y., M. W. Wu, Q. S. Ge, et al., 2017: Observed, reconstructed, and simulated decadal variability of summer precipitation over eastern China. *J. Meteor. Res.*, **31**, 49–60, doi: 10.1007/s13351-017-6115-5.

Zhou, X. C., D. B. Jiang, and X. M. Lang, 2020: Unstable relationship between the Pacific Decadal Oscillation and eastern China summer precipitation: Insights from the Medieval Climate Anomaly and Little Ice Age. *Holocene*, **30**, 799–809, doi: 10.1177/0959683620902215.

Zhou, Y. F., and Z. W. Wu, 2016: Possible impacts of mega-El Niño/Southern Oscillation and Atlantic Multidecadal Oscillation on Eurasian heatwave frequency variability. *Quart. J. Roy. Meteor. Soc.*, **142**, 1647–1661, doi: 10.1002/qj.2759.

Zhu, Y. M., and X. Q. Yang, 2003: Relationships between Pacific Decadal Oscillation (PDO) and climate variabilities in China. *Acta Meteor. Sinica*, **61**, 641–654, doi: 10.3321/j.issn:0577-6619.2003.06.001. (in Chinese)

Tech & Copy Editor: Mengyuan CHEN

Journal of Meteorological Research

Vol. 35 No. 5 October 2021

CONTENTS

Journal of Meteorological Research

http://jmr.cmsjournal.net

http://link.springer.com/journal/13351

ISSN 2095-6037

9 772095 603213 10>